probably line the ion incursion channels where migration of PQ^{2+} and diffusional quenching are both rapid. One effect of added TEOA is to increase the fraction of chromophores available to PQ^{2+} in this region by swelling the polymeric matrix. (3) The slow-quenching component at site 2 is buried within the hydrophobic, unhydrolyzed portion of the film where the concentration of [PQ](ClO$_4$)$_2$ is low and diffusion slow. The addition of [NEt$_4$](ClO$_4$) apparently enhances the rate of ionic diffusion by PQ^{2+} in this region, and excited-state quenching, although slow, does occur. (4) Those sites that are unquenchable are shown as being deeply buried within the hydrophobic region. They may lie in domains of relatively high local crystallinity where diffusion of PQ^{2+} is slow on the time scale for the excited-state decay.

Acknowledgment. We acknowledge support of this research from the Department of Energy under Grant No. DE-AS05-78ER06034.

Registry No. [(bpy)$_2$Ru(5-NH$_2$phen)]$^{2+}$, 84537-85-9; [(bpy)$_2$Ru(5-N(p-SO$_2$C$_6$H$_4$CH$_3$)$_2$phen)]$^{2+}$, 117024-07-4; 5-N(p-SO$_2$C$_6$H$_4$CH$_3$)$_2$phen, 116996-87-3; 6,7-dihydrodipyrido[1,2-a:2′,1′-C]pyrazinediium, 2764-72-9; (E)-bis[1-methylpyridinium]-4,4′-(1,2-ethenediyl), 46740-72-1; 1,1′-dimethyl-4,4′-bipyridinium, 4685-14-7; 6,7-dihydro-2,11-dimethyldipyrido[1,2-a:2′,1′-C]pyrazinediium, 16651-71-1; 7,8-dihydro-6H-dipyrido[1,2-a:2′,1′-C][1,4]diazepinediium, 7325-63-5; 6,7,8,9-tetrahydrodipyrido[1,2-a:2′,1′-C][1,4]diazocinediium, 16651-68-6; 7,8-dihydro-2,12-dimethyl-6H-dipyrido[1,2-a:2′,1′-C][1,4]diazepinediium, 16651-74-4.

Photoeffects in Thin-Film Molecular-Level Chromophore–Quencher Assemblies. 2. Photoelectrochemistry

Nigel A. Surridge, Joseph T. Hupp, Stephen F. McClanahan, Sharon Gould, and Thomas J. Meyer*

Department of Chemistry, The University of North Carolina, Chapel Hill, North Carolina 27599-3290

(Received: June 1, 1987; In Final Form: June 22, 1988)

Photocurrents appear upon visible photolysis of thin films of chlorosulfonated polystyrene ([–CH$_2$CH(p-C$_6$H$_4$SO$_2$Cl)]$_x$–; PS–SO$_2$Cl) containing the chemically attached chromophore [(bpy)$_2$Ru(5-NH$_2$phen)](PF$_6$)$_2$ (bpy is 2,2′-bipyridine, 5-NH$_2$phen is 5-amino-1,10-phenanthroline). The chemical attachment is by sulfonamide binding. The photocurrents arise following oxidative quenching of the metal-to-ligand charge-transfer excited state(s) of the complex by paraquat (PQ^{2+}) in the presence of the reductive scavenger TEOA, triethanolamine. A kinetic model has been derived that accounts for variations in photocurrent with light intensity and [PQ^{2+}] or [TEOA] in the external solution. Comparisons with earlier quenching studies obtained by laser flash photolysis show that only a fraction of the chromophores in the film contribute to the photocurrent. The efficiency of photocurrent production depends upon the concentration gradient of the chromophore. It rises initially as the chromophore content increases but falls dramatically in films where the chromophore has reached the electrode–film interface. Under maximal conditions the per photon absorbed quantum yield for photocurrent production reaches 0.14, 0.18 with 0.1 M isopropyl alcohol added.

Introduction

In previous papers,[1-3] the preparation and characterization of thin polymeric films of chlorosulfonated polystyrene (PS–SO$_2$Cl) were described in which the metal-to-ligand charge-transfer (MLCT) chromophore [(bpy)$_2$Ru(5-NH$_2$phen)]$^{2+}$ (bpy is 2,2′-bipyridine; 5-NH$_2$phen is 5-amino-1,10-phenanthroline)

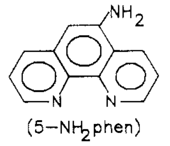

(5–NH$_2$phen)

was incorporated by chemical binding:

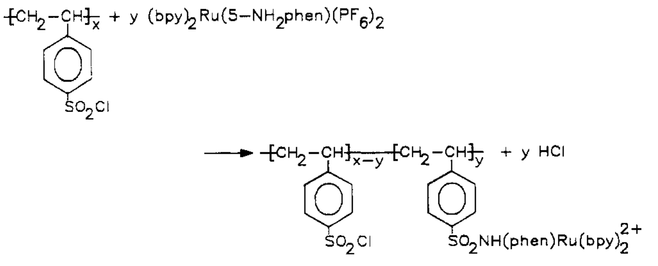

$$\{CH_2-CH(C_6H_4SO_2Cl)\}_x + y\,(bpy)_2Ru(5\text{-}NH_2phen)(PF_6)_2 \longrightarrow \{CH_2-CH(C_6H_4SO_2Cl)\}_{x-y}\{CH_2-CH(C_6H_4SO_2NH(phen)Ru(bpy)_2^{2+})\}_y + y\,HCl$$

[(bpy)$_2$Ru(5–NH(SO$_2$–PS)phen)]$^{2+}$

From the results of a series of photophysical and quenching studies in the presence of the oxidative quencher PQ^{2+} (paraquat)[1]

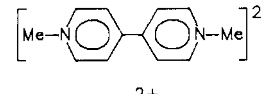

(PQ^{2+})

a number of conclusions were reached concerning the physical structure of the resulting films: (1) Following partial hydrolysis, which converts <5% of the unreacted –SO$_2$Cl sites into –SO$_3^-$ ion-exchange sites, PQ^{2+} is concentrated within the films. (2) Partial hydrolysis appears to create ion-exchange incursion channels that allow PQ^{2+} to reach and quench a high percentage of the chromophoric sites. (3) Following the hydrolysis step, the Ru-based chromophore occupies three distinctly different chemical sites. The first site is near the ion-exchange incursion channels where rapid quenching by PQ^{2+} occurs. The second is in a hydrophobic region where relatively slow quenching occurs and then only with added [NEt$_4$](ClO$_4$) as an ion carrier. The third site remains unquenched even at high quencher concentrations and may be in the hydrophobic region in a domain of relatively high local crystallinity.

As constituted, the films contain a chromophore–quencher apparatus, reactions 1 and 2, which has been used frequently in

$$(bpy)_2Ru(5\text{-}NH(SO_2\text{–}PS)phen)^{2+} \xrightarrow{h\nu} (bpy)_2Ru(5\text{-}NH(SO_2\text{–}PS)phen)^{2+*} \quad (1)$$

$$(bpy)_2Ru(5\text{-}NH(SO_2\text{–}PS)phen)^{2+*} + PQ^{2+} \rightarrow (bpy)_2Ru(5\text{-}NH(SO_2\text{–}PS)phen)^{3+} + PQ^{+} \quad (2)$$

$$(bpy)_2Ru(5\text{-}NH(SO_2\text{–}PS)phen)^{3+} + PQ^{+} \rightarrow (bpy)_2Ru(5\text{-}NH(SO_2\text{–}PS)phen)^{2+} + PQ^{2+}$$

---

(1) Surridge, N. A.; McClanahan, S. F.; Hupp, J. T.; Danielson, E.; Meyer, T. J. *J. Phys. Chem.*, preceding article in this issue.

(2) (a) Hupp, J. T.; Otruba, J. P.; Parus, S. J.; Meyer, T. J. *J. Electroanal. Chem.* **1985**, *190*, 287. (b) Hupp, J. T.; Meyer, T. J. *J. Electroanal. Chem.*, in press. (c) Hupp, J. T.; Meyer, T. J., submitted for publication.

(3) Ellis, C. D.; Meyer, T. J. *Inorg. Chem.* **1984**, *23*, 1748.

0022-3654/89/2093-0304$01.50/0

solution.[4] However, in the films there is the distinctive feature that the chromophore occupies a fixed site while the quencher couple is mobile and, further, that the distribution of the chromophore within the films can be varried systematically given the nature of the attachment chemistry.

Photoeffects have been observed in other polymeric film-based systems containing fixed-site chromophores.[2,5] One of our goals is to learn how to manipulate the microstructures within such films. With appropriately designed microstructures it should be possible to mimic the p/n junction of a semiconductor-based photodiode or the excitation/quenching/electron transfer sequence that leads to redox splitting in the photosynthetic reaction center. With this goal in mind, the chlorosulfonated films offer a great deal of flexibility synthetically. The intention here was first to assemble a molecular photochemical apparatus in PS–SO_2Cl films for the production of oxidative and reductive equivalents. Second, we wished to begin to learn how to utilize structural effects to transfer those equivalents to spatially separated regions within the film.

Experimental Section

Materials. The materials used were as described in the previous paper.[1]

Film Preparation. For the work reported here, films were prepared either by evaporative deposition on Teflon-shrouded Pt or glassy carbon electrodes[1] or by spin casting onto flat electrode substrates. In the latter procedure, precut squares of barium borosilicate glass, which were used as a substrate (1.14 × 1.14 × 0.04 cm; Corning 7059 from F. G. Gray Co.), were subjected to a stream of high-pressure air to remove dust, rinsed with distilled water, transferred (without drying) to an isopropanol solution, and sonicated for 30 min. The glass was suspended above a second solution of refluxing isopropanol for a minimum of 12 h and, after cooling and drying in the isopropanol atmosphere, transferred rapidly to a Veeco VE 300 evaporator. The glass squares were partially masked by an aluminum template, leaving uncovered a central circle 4 mm in diameter together with a 2-mm wide strip along one edge and a connecting strip between the edge and center circle. A 1000–2000-Å-thick film of Ti was evaporatively deposited onto the unmasked portions of the glass to act as an anchor for the subsequent layer of Pt (1000 Å), which rendered the surface conductive. The Pt layer was deposited with a Polaron SEM E5100 sputter coater. At all stages of substrate preparation, care was taken to minimize dust contamination.

Polymeric films were cast under inert-atmosphere conditions with a Vacuum Atmospheres Model HE-493 inert-atmosphere box by dropping ~10 μL of a solution containing a known quantity of PS–SO_2Cl in 2-butanone (Aldrich) onto a spinning slide (2000 rpm; Headway Research Spin Coater) and allowing it to evaporate. By variation of the concentration of the polymer in the solution between 80 and 400 mM, controlled film thicknesses of between 450 and 3000 Å were obtained. The most uniform films were obtained for thicknesses ≤1000 Å. The thicknesses were measured by using surface profilometry (Tencor Alpha-Step 100 step profiler) and were found to vary by no more than ±15% when measured on various parts of the same sample. The reproducibility from one sample to another, with the same spin casting conditions, was ±40%. The films were vacuum dried at room temperature for 2 h, and the time of exposure to air prior to the incorportion of the chromophore was minimized.

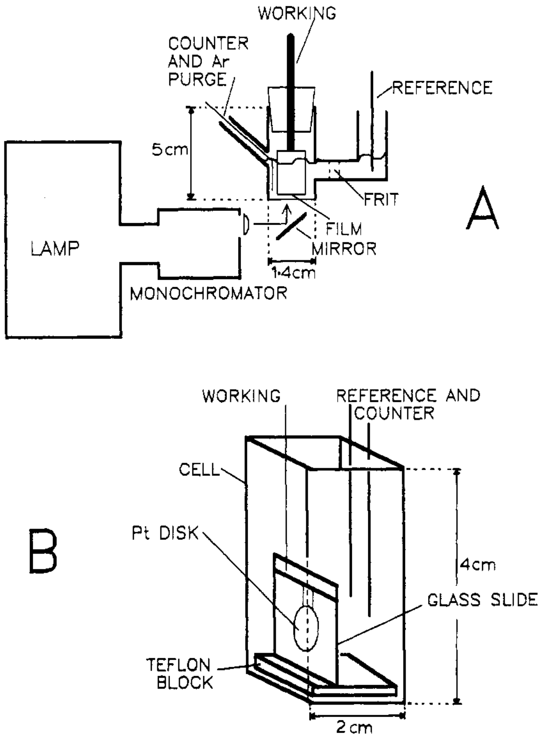

Figure 1. Photoelectrochemical cells for film photocurrent measurements: (A) for films drop-coated onto 0.125-cm^2 platinum button electrodes and for actinometry experiments; (B) for films spun cast onto a 0.28-cm^2 area of platinum sputter coated on to a glass substrate.

Incorporation of the Chromophore. The chromophore was incorporated into the films by soaking the film coated electrodes in acetonitrile solutions 5 mM in $[(bpy)_2Ru(5\text{-}NH_2phen)]^{2+}$ for varying lengths of time. Small amounts of the polymer appear to be lost by dissolution during the time that films are soaked in acetonitrile solutions containing the chromophore. However, infrared analysis of the residues of these solutions showed that the quantity lost is small. In experiments where films were soaked for varying periods of time, the difference in the amount lost was accounted for by light-absorbance measurements *after* incorporation of the chromophores.

Hydrolysis of the Film. Immediately following incorporation of the chromophore, films were transferred without drying to a 0.5 M $NaHCO_3/Na_2CO_3$ buffer solution (pH ~9.6) and allowed to hydrolyze partially for 3.5 h before soaking in distilled water for ≥10 min. This was followed by a brief rinse with acetonitrile and soaking in 0.1 M $[Et_4N](ClO_4)$/acetonitrile for ≥15 min prior to transfer to the experimental solution. The final step removes any unbound ruthenium complex, presumably by a swelling of the membrane by added $[NEt_4](ClO_4)$ (TEAP).

Measurements. For the photoelectrochemical measurements, the light source was a Hanovia 1000-W Hg/Xe lamp or a Bausch and Lomb 200-W Hg lamp coupled to a Bausch and Lomb high-intensity monochromator (1350 grooves/mm) equipped with variable slits. Solutions were continuously purged with solvent-saturated argon. Two different cell arrangements were used, the choice depending on the type of film used. For evaporatively deposited films on Pt electrodes, the cell was arranged so that the light output of the monochromator was deflected vertically, thereby entering the bottom of the cell and irradiating the polymer film–electrode assembly, which was secured in a vertical position by a brass shaft that was threaded into the working electrode and held by a Teflon thermometer adapter as shown in Figure 1A. A small side arm in the cell allowed for both the Pt wire counter electrode and the Ar purge tube. A coarse sintered glass frit

---

[4] (a) Bock, C. R.; Meyer, T. J.; Whitten, D. G. *J. Am. Chem. Soc.* **1974**, *96*, 4710. (b) Balzani, V.; Bolleta, F.; Gandolfi, M. T.; Maestri, M. *Top. Curr. Chem.* **1978**, *75*, 1. (c) Kalyanasundaram, K. *Coord. Chem. Rev.* **1982**, *46*, 159. (d) Meyer, T. J. *Prog. Inorg. Chem.* **1983**, *30*, 389. (e) Bock, C. R.; Connor, J. A.; Guttierez, A. R.; Meyer, T. J.; Whitten, D. G.; Sullivan, B. P.; Nagle, J. K. *J. Am. Chem. Soc.* **1979**, *101*, 4815. (f) Durham, B.; Dressick, W. J.; Meyer, T. J. *J. Chem. Soc., Chem. Commun.* **1979**, 381. (g) Moradpour, A.; Amouyal, E.; Keller, P.; Kagan, H. *Nouv. J. Chim.* **1978**, *2*, 547. (h) Young, R. C.; Meyer, T. J.; Whitten, D. G. *J. Am. Chem. Soc.* **1975**, *97*, 4781. (i) Sutin, N. *J. Photochem.* **1979**, *10*, 19. (j) Sutin, N.; Creutz, C. *Pure Appl. Chem.* **1980**, *52*, 2717.

[5] (a) Kaneko, M.; Yamada, A. *Electrochim. Acta* **1986**, *31*, 273. (b) Kaneko, M.; Moriya, S.; Yamada, A.; Yamamoto, H.; Oyama, N. *Electrochim. Acta* **1984**, *29*, 115. (c) Oyama, N.; Yamaguchi, S.; Kaneko, M.; Yamada, A. *J. Electroanal. Chem.* **1982**, *139*, 215. (d) Wohrle, D.; Bannehr, R.; Schumann, B.; Meyer, G.; Jaeger, N. *J. Mol. Catal.* **1983**, *21*, 255. (e) Tamilarasan, R.; Ramaraj, R.; Subramanian, R.; Natarajan, P. *J. Chem. Soc., Faraday Trans. 1* **1984**, *80*, 2405. (f) Margerum, L. D.; Murray, R. W.; Meyer, T. J. *J. Electroanal. Chem.* **1983**, *149*, 279. (g) Westmoreland, T. D.; Calvert, J. M.; Murray, R. W.; Meyer, T. J. *J. Chem. Soc., Chem. Commun.* **1983**, 65.

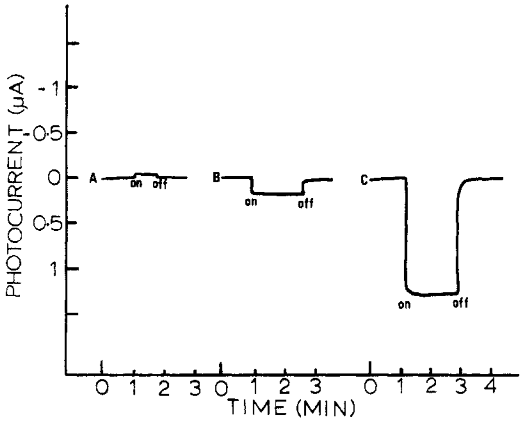

Figure 2. Photocurrent–time curves produced by photolysis (λ_{exc} = 436 nm; $I_0 = 6.6 \times 10^{-9}$ einstein cm^{-2} s^{-1}) of PS–SO_2Cl (10 μL of a 0.4 mg/mL actone solution) evaporatively cast onto a 0.125-cm^2 Pt button electrode, soaked in 5 mM [$(bpy)_2Ru(5\text{-}NH_2phen)$][$PF_6$]$_2$ for 2 h followed by hydrolysis in 0.5 M $NaHCO_3/Na_2CO_3$ for 3.5 h: (A) with only 0.1 M TEAP/acetonitrile in the external solution; (B) with 60 mM triethanolamine (TEOA) added to (A); (C) with both TEOA and 0.25 mM PQ^{2+} added.

connected the cell to the reference electrode compartment.

The small cell arrangement was used for the quantum yield measurements. For the quantum yield measurements the incident light intensity was determined by ferrioxalate actinometry.[6] The photoelectrochemical and actinometry measurements were determined by using the same cell with care taken to align the cell at the same position in the optical train for both types of experiments. For the actinometry measurements the cell was masked with aluminum foil except for a circular area on the bottom face having the same surface area as the electrodes used in the quantum yield determination. For the actinometry measurements the cell was filled with sufficient ferrioxalate solution (0.15 M) to give an optical path length of 2 cm. So that problems arising from cross-sectional inhomogeneities in the light beam could be avoided, care was taken to irradiate with the same part of the beam for both types of experiments.

For spun-cast films the light beam entered the side of a square Pyrex cell directly and was focused onto a Pt/polymer disk centered on a glass slide as shown in Figure 1B. The slide was held in position 1 mm from the cell wall by a Teflon block in the bottom of the cell. Electrical contact was made to the electrode at the platinum bar with a platinum wire and gold epoxy resin (Epo-Tech) which was insulated from solution by nonconducting epoxy resin. Reference and counter electrodes along with the Ar purge tube were placed in the solution behind the glass slide. All potentials are reported versus the sodium chloride calomel electrode (SSCE).

In a series of experiments the spatial distribution of the chromophore within the polymeric films from the film–solution interface to the electrode–film interface was varied by soaking a series of identically prepared films in the chromophore-containing solution for varying periods of time. Analyses of the resulting spatial distributions were carried out by secondary ionization mass spectrometry (SIMS) with an O_2^+ ion beam microprobe. The procedures used and results obtained have appeared elsewhere.[7]

In experiments involving the quantitative photoelectrochemical response of the films, the photocurrents cited are plateau values after the photoelectrochemical response had reached a steady state (note Figure 2).

Results

Analysis. In the presence of the oxidative quencher PQ^{2+} and the reductive scavenger triethanolamine ($N(C_2H_4OH)_3$, TEOA), the excitation, reaction 3, electron-transfer quenching, reaction 4, back electron transfer, reaction 5, and scavenging steps, reaction 6, proposed in Scheme I are known to operate for $[Ru(bpy)_3]^{2+}$.[4]

SCHEME I

in the film

$$(bpy)_2Ru^{II}(5\text{-}NH(SO_2\text{–}PS)phen)^{2+} \xrightarrow[1/\tau = k_r + k_{nr}]{h\nu} (bpy)_2Ru^{III}(5\text{-}NH(SO_2\text{–}PS)phen^{\bullet -})^{2+*} \quad (3)$$

$$(bpy)_2Ru^{III}(5\text{-}NH(SO_2\text{–}PS)phen^{\bullet -})^{2+*} + PQ^{2+} \xrightarrow{k_q\phi_{sep}} (bpy)_2Ru^{III}(5\text{-}NH(SO_2\text{–}PS)phen)^{3+} + PQ^{\bullet +} \quad (4)$$

$$(bpy)_2Ru^{III}(5\text{-}NH(SO_2\text{–}PS)phen)^{3+} + PQ^{\bullet +} \xrightarrow{k_b} (bpy)_2Ru^{II}(5\text{-}NH(SO_2\text{–}PS)phen)^{2+} + PQ^{2+} \quad (5)$$

$$(bpy)_2Ru^{III}(5\text{-}NH(SO_2\text{–}PS)phen)^{3+} + N(C_2H_4OH)_3 \xrightarrow{k_s} (bpy)_2Ru^{II}(5\text{-}NH(SO_2\text{–}PS)phen)^{2+} + N(C_2H_4OH)_3^{\,+} \quad (6)$$

$$N(C_2H_4OH)_3^{\,+} \rightarrow \frac{1}{2}N(C_2H_4OH)_3 + \frac{1}{2}(HOC_2H_4)_2NCH_2CHO + H^+ \quad (7)$$

at the inner electrode

$$PQ^{\bullet +} \xrightarrow[k_a]{-e^-} PQ^{2+} \quad (8)$$

$$(bpy)_2Ru^{III}(5\text{-}NH(SO_2\text{–}PS)phen)^{3+} \xrightarrow[k'_a]{+e^-} (bpy)_2Ru^{II}(5\text{-}NH(SO_2\text{–}PS)phen)^{2+} \quad (9)$$

Scheme I is different from analogous solution cases in that the chromophore, $[(bpy)_2Ru(5\text{-}NH(SO_2\text{–}PS)phen)]^{2+}$, occupies chemically fixed sites within the films and is *not* diffusionally mobile. In eq 4 the rate constant for the appearance of the photoproduced oxidative (Ru(III)) and reductive (PQ^+) redox equivalents is written as the product of a quenching rate constant, k_q, and a separation efficiency, ϕ_{sep}, as will be discussed. The PQ^{2+} quenching step within the films has been investigated by emission quenching techniques.[1] The existence of the remaining steps is at least qualitatively consistent with variations in the photocurrent with light intensity, [PQ^{2+}], [TEOA], and soaking time as described below.

The net photochemical reaction in Scheme I is

$$PQ^{2+} + \tfrac{1}{2}N(C_2H_4OH)_3 + h\nu \rightarrow PQ^+ + \tfrac{1}{2}(HOC_2H_4)_2NCH_2CHO + H^+ \quad (10)$$

In the scheme it is assumed that when oxidized, triethanolamine reaches the aldehyde product by disproportionation of $TEOA^+$.[8] A second possibility is that the intermediate TEOA radical undergoes a further 1-e$^-$ oxidation by PQ^{2+} to give the aldehyde and a second PQ^+ in a following reaction. In any case, the photochemically produced reductive equivalents are delivered to the electrode as PQ^+ at applied potentials more positive than the formal potential of the $PQ^{2+/+}$ couple (−0.44 vs SSCE). The oxidizing equivalents, which appear initially as Ru(III), ultimately appear in the external solution as oxidized TEOA. In reaction 10 the oxidation of TEOA by PQ^{2+} is sensitized by the chemically bound Ru–bpy chromophore in the film.

The quenching of the excited state by PQ^{2+} and the scavenging of Ru(III) by TEOA both occur within the film. PQ^{2+} and TEOA are introduced into the external solution and diffuse into the film. In general, the magnitude of the experimentally observed photocurrent should depend upon both the rate of photochemically produced redox equivalents (i_p) and the slower of the two rates of diffusion into the films (i_D). In the limit that electron transfer to the electrode via the $PQ^{2+/+}$ couple is rapid, the experimentally observed photocurrent, $i_{h\nu}$, is given by

---

(6) Calvert, J. G.; Pitts, J. N. *Photochemistry*; Wiley: New York, 1966; p 783.

(7) Surridge, N. A.; Linton, R. W.; Hupp, J. T.; Bryan, S. R.; Meyer, T. J.; Griffis, D. P. *Anal. Chem.* **1986**, *58*, 2443.

(8) Kalyanasundaram, K.; Kiwi, J.; Gratzel, M. *Helv. Chim. Acta* **1978**, *61*, 2720.

$$\frac{1}{i_{h\nu}} = \frac{1}{i_p} + \frac{1}{i_D} \qquad (11)$$

With 0.1 M TEAP–CH_3CN in the external solution, PQ^{2+} is concentrated within the films with a partition constant of $\sim 10^2$.[1] The $PQ^{2+/+}$ couple acts as an electron-transfer carrier and is not depleted in the photoelectrochemical cycle. However, TEOA is depleted, and contributions to the photocurrent from diffusion are expected to be dominated by TEOA.

Assuming linear diffusion, the current on the diffusion plateau for a stirred solution voltammogram is given by eq 12.[9]

$$|i| = nFAD(C/x) \qquad (12)$$

In eq 12, D is the diffusion coefficient in $cm^2\ s^{-1}$, A is the electrode area in cm^2, F is the Faraday constant, n is the electrochemical stoichiometry, C is the bulk concentration of the electroactive form of the couple, and x is the thickness of the diffusion layer. In the photoelectrochemical experiment the electroactive species (PQ^+) is replenished by the molecular photochemical apparatus within the film rather than by stirring.

In the limit that the concentration gradient is steep and the concentration of PQ^{2+} and TEOA in the external solution sufficiently high that $i_D \gg i_p$, eq 11 becomes

$$i_{h\nu} = i_p$$

In the limit that the photocurrent response is dictated by i_p, the magnitude of $i_{h\nu}$ will be determined by one or more of the individual steps in Scheme I.

For want of detailed information concerning the interior structure of the films, we will assume the linear diffusion model of eq 12 in analyzing the photocurrents. The goal is not to develop a quantitative model for the photocurrents but rather to understand the trends that occur when $[PQ^{2+}]$, [TEOA], or the light intensity is varied.

When the photocurrent reaches a plateau (Figure 2), the rates of production of PQ^+ by the photochemical molecular apparatus and depletion by oxidation at the inner electrode are equal and $[PQ^+]$ reaches a photostationary state, $[PQ^+]_{PSS}$. Assuming linear diffusion and eq 12, the photocurrent is given by eq 13.

$$i_{h\nu} = nFAD_{PQ^+}[PQ^+]_{PSS}/x \qquad (13)$$

It is possible to derive a steady-state expression for $[PQ^+]_{PSS}$ based on the sequence of coupled reactions in Scheme I. The result shown in eq 14 was derived by assuming the validity of the

$$[PQ^+] = \frac{C_1 I_0}{1 + (1 + C_2 I_0/[TEOA])^{1/2}} \qquad (14)$$

$$C_1 = \frac{2(1 - 10^{-A_T})(A_{Ru}/A_T)\phi_q\phi_{sep}}{k_{ct}} \qquad (14a)$$

$$C_2 = \frac{4(1 - 10^{-A_T})(A_{Ru}/A_T)\phi_q\phi_{sep}k_b}{k_{ct}k_s} \qquad (14b)$$

steady-state approximation for Ru(III) and PQ^+ and neglects direct reduction of Ru(III) at the electrode by reaction 9. As will be shown, the latter assumption is valid only for films in which the chromophore has not reached the inner electrode. In eq 14 $[PQ^+]$ and $[PQ^+]_{PSS}$ are taken to be the same. It follows from eq 13 and 14 that the photocurrent is given by

$$i_{h\nu} = nFAD_{PQ^+}\frac{[PQ^+]}{x} = \left(\frac{nFAD_{PQ^+}}{x}\right)\frac{C_1 I_0}{1 + (1 + C_2 I_0/[TEOA])^{1/2}} \qquad (15)$$

The photocurrent density, $j_{h\nu}$, is related to $i_{h\nu}$ by

$$j_{h\nu} = i_{h\nu}/A$$

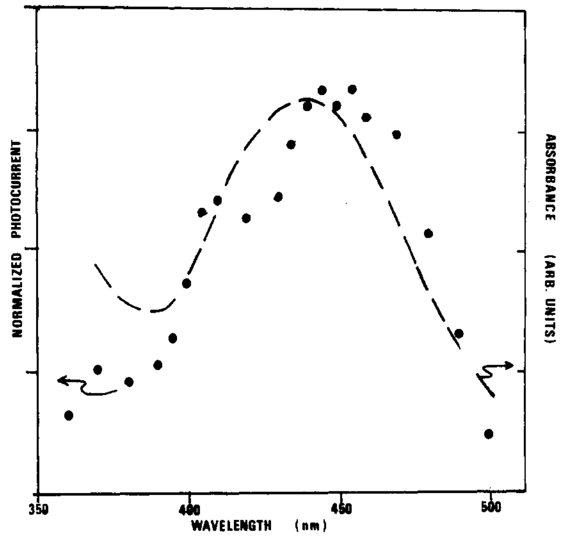

Figure 3. Point-by-point photocurrent action spectrum obtained by using the conditions of Figure 2. The absorption spectrum in the same spectral region after dissolving the film in dimethyl sulfoxide is shown in the dashed line. The photocurrent action spectrum was corrected for variations in lamp intensity by using a power meter.

The following quantities appear in eq 14 and 15:

$i_{h\nu}$	photocurrent, A
n	electrochemical stoichiometry
F	Faraday's constant
A	area of electrode, cm^2
I_0	incident light intensity, einsteins $cm^{-2}\ s^{-1}$
A_T	total absorbance of the cell
A_{Ru}	absorbance by the chromophore
$1 - 10^{-A_T}$	fraction of incident light intensity absorbed by the cell
A_{Ru}/A_T	fraction of light absorbed by the chromophore
ϕ_q	quenching efficiency. In terms of the constants in Scheme I, $\phi_q = k_q[PQ^{2+}]/(k_q[PQ^{2+}] + 1/\tau)$
ϕ_{sep}	separation efficiency. The fraction of [Ru(III),PQ^+] pairs produced in the quenching step that lead to separate redox products (eq 25)
k_s	rate constant for reduction of Ru(III) by TEOA
k_b	back electron transfer rate constant for the reduction of Ru(III) by PQ^+ *after* they have separated out of th [Ru(III),PQ^+] pair

From eq 15 and Scheme I the magnitude of the photocurrent is determined by four factors: the number of moles of photons absorbed by the chromophore per unit time $I_0(1 - 10^{-A_T})(A_{Ru}/A_T)$, the two efficiencies ϕ_q and ϕ_{sep}, and the competition for Ru(III) between PQ^+, TEOA, and the electrode, the latter assumed to be negligible at least initially. Equation 15 provides a semiquantitative basis for describing the photoelectrochemical response when $i_{h\nu} = i_p$.

Film-Based Photoelectrode. Irradiation into the MLCT absorption bands of the Ru-based chromophore in a chlorosulfonated polystyrene film on Pt or carbon electrodes with added PQ^{2+} and triethanolamine in CH_3CN leads to significant photocurrents. The currents are independent of the nature of the substrate electrode and persist relatively unchanged (±10%) for periods greater than 1 h. A typical short-time response for an evaporatively cast film is shown in Figure 2. In the absence of PQ^{2+} and TEOA, a small reductive current is observed (Figure 2A). If the solution is also made 60 mM in TEOA a somewhat larger, oxidative current is observed (Figure 2B). The oxidative current is greatly enhanced by the addition of PQ^{2+} (Figure 2C). Figure 3 shows a point-by-point photocurrent action spectrum for an identically prepared electrode. The action spectrum follows the absorption spectrum of the chromophore reasonably well.

The magnitude of the photocurrent is independent of the applied potential in the range +0.2 to −0.3 V vs SSCE. It decreases as the applied potential nears the formal potential of the $PQ^{2+/+}$

---

(9) Bard, A. J.; Faulkner, L. R. *Electrochemical Methods*; Wiley: New York, 1980; p 29.

couple at −0.44 V, where the background current for the $PQ^{2+/+}$ couple begins to interfere. At potentials that are too positive, direct oxidation of TEOA at the electrode interferes. Other properties of the photoelectrode include (1) the sense of the photocurrent ($i_{h\nu}$) is oxidative, (2) the magnitude of $i_{h\nu}$ increases with increasing [TEOA] and [PQ^{2+}] (see below), (3) from the lifetime results, which were presented earlier,[1] PQ^{2+} is known to quench at least a fraction of the Ru-based excited states in the films. Where comparisons have been made, equivalent results have been obtained for the macroscopically rough, evaporatively cast films and the smoother, spatially more homogeneous spun-cast films on carbon or Pt electrodes.

Variations in $j_{h\nu}$ *with* [PQ^{2+}], *[TEOA], and* I_0. The experiments described above show that the photoresponse of the films is at least qualitatively consistent with Scheme I. We have explored the variation of $j_{h\nu}$ with [PQ^{2+}], [TEOA], and I_0 in further detail. In these experiments a constant soaking time of ~2 h was used for the incorporation of the chromophore. As noted in a later section, $j_{h\nu}$ is strongly dependent upon the soaking time and, by inference, upon the concentration distribution of the chromophore within the films.

Quenching Efficiency. In solution the quantum efficiency for oxidative electron-transfer quenching is given by eq 16, where K_{SV}

$$\phi_q = K_{SV}[PQ^{2+}]/(1 + K_{SV}[PQ^{2+}]) \qquad (16)$$

is the Stern–Volmer constant. It is the product of the quenching rate constant (k_q) and the excited state lifetime (τ).

The quenching dynamics within the film environment are potentially far more complicated than in solution since (1) there is experimental evidence that the chromophores occupy three different chemical sites within the films, one of which is quenched rapidly, one slowly, and one not at all;[1] (2) in each of the three sites the chromophores decay nonexponentially;[1] (3) in the photoelectrochemical experiment the quenching event is monitored indirectly by the appearance of a photocurrent at the inner electrode. The inner electrode is relatively remote from the chromophoric sites. They are concentrated in the outside of the films; see below.

At high concentrations of TEOA and low incident-light intensities, the term (C_2I_0/[TEOA]) → 0 in eq 15. Under these conditions capture of Ru(III) by PQ^+ is negligible and scavenging by TEOA is complete. Assuming that, once formed, transport of PQ^+ to the electrode is rapid, eq 15 leads to

$$j_{h\nu} = nFI_0(1 - 10^{-A_T})(A_{Ru}/A_T)\phi_q\phi_{sep} \qquad (17)$$

where $k_{ct} = D_{PQ^+}/x$. The inverse of eq 17 is

$$j_{h\nu}^{-1} = (1 + 1/K_{SV}[PQ^{2+}])C_3 \qquad (18a)$$

$$C\;^{-1} = nFI_0(1 - 10^{-A_T})(A_{Ru}/A_T)\phi_{sep} \qquad (18b)$$

Equation 18 was derived earlier for a related solution-based photocell but without properly taking into account the competition between PQ^+ and TEOA for Ru(III).[10] The earlier treatment is valid in the limit that capture of Ru(III) by TEOA is complete with no competition from back electron transfer by PQ^+.

The assumption that the oxidation of PQ^+ is rapid appears to be justified under our conditions. The electrochemical reduction of PQ^{2+} to PQ^+ through the films was observed in a series of rotated-disk experiments. In the experiments the limiting current was measured at rotation rates ranging from 400 to 3500 rpm. Levich plots of the limiting current, i_l, vs the square root of the rotation rate, $\omega^{1/2}$, show a negative deviation from linearity with increasing rotation rates. This indicates that mass transport of PQ^{2+} through the film begins to limit the reduction current at high rotation rates. The maximum value of the mass-transport-limited current, as given by the inverse of the intercept of a Koutecky–Levich plot of i_l^{-1} vs $\omega^{-1/2}$, was ~40 times higher than the highest value of $i_{h\nu}$ in the photochemical experiments.

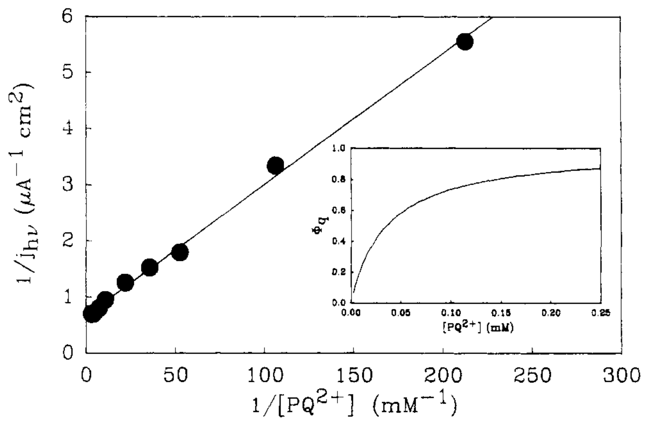

Figure 4. Plot of the inverse of the photocurrent density, $j_{h\nu}^{-1}$ vs $[PQ^{2+}]^{-1}$ (see eq 18a) at λ_{exc} = 436 nm. As in Figure 2 with 0.1 M TEAP and 10^{-2} M TEOA in the external solution and $I_0 \sim 10^{-9}$ einstein cm^{-2} s^{-1}. Shown in the inset is the quenching efficiency (ϕ_q) as a function of quencher concentration, which was calculated by using eq 16 and $K_{SV} = 2.3 \times 10^4$ M^{-1}.

In Figure 4 is shown a plot of $j_{h\nu}^{-1}$ vs $[PQ^{2+}]^{-1}$ for a film soaked for 2 h in $(bpy)_2Ru(5\text{-}NH_2phen)^{2+}$ and placed in a cell containing 100 mM TEOA. From this and repeated experiments there appears to be a slight curvature with an increasing slope at higher concentrations of PQ^{2+}. The curvature suggests that we were unable to achieve conditions where C_2I_0/[TEOA] is completely negligible. Nonetheless, estimates of K_{SV} were made by fitting straight lines to data such as those shown in Figure 4. The extent of deviation from linearity is expected to be greatest at high [PQ^{2+}]. As [PQ^{2+}] increases, the extent of quenching and the steady-state concentration of PQ^+ both increase.

In six separate experiments at [TEOA] = 1.0 M or 100 mM and at varying light intensities, K_{SV} varied from 1.0×10^4 to 3.0×10^4 M^{-1} with an average value of 2.3×10^4 M^{-1}. A plot of ϕ_q vs [PQ^{2+}] calculated by using this value of K_{SV} and eq 16 is shown in the inset to Figure 4.

If the film hydrolysis step is omitted or shortened in the preparation sequence, photocurrents are reduced and the inverse–inverse plots become radically less linear. The nearly Stern–Volmer behavior observed in Figure 4 shows that excited-state quenching is dynamic rather than static in nature, at least in the hydrolyzed films.

In the earlier laser flash photolysis experiments evidence was found for three different chromophoric sites which were quenched at significantly different rates.[1] In the photocurrent experiments, which were carried out under identical conditions, there is evidence for only a single quenching process. That process is essentially independent of added $[NEt_4](ClO_4)$, and its Stern–Volmer constant is the same within experimental error as the value obtained for the most rapidly quenched of the three components identified in the lifetime experiments ($K_{SV} \sim 3.2 \times 10^4$ M^{-1}).[1] The comparisons show that only the most rapidly quenched site contributes to the photocurrent. They also suggest that in experiments such as that in Figure 4, we are close to a domain where eq 17 is valid, at least at low [PQ^{2+}].

The calculation of k_q from the experimental Stern–Volmer constants is complicated by two factors. PQ^{2+} is concentrated in the partially hydrolyzed films with $K_p = [PQ^{2+}]_{film}/[PQ^{2+}]_{solution} \approx 10^2$.[1] With the effect of partitioning included, $K_{SV} = k_q\tau K_p$, and $k_q = K_{SV}(\tau K_p)^{-1}$. In addition, the film-based excited states decay nonexponentially. The intensity–time profile of the component that contributes to the photocurrent can be fit satisfactorily to the biexponential function

$$I(t) = A_1\exp(-t/\tau_1) + A_2\exp(-t/\tau_2)$$

with τ_1 = 700 ns, τ_2 = 115 ns, and A_2/A_1 = 3.75 at 25 °C in 0.1 M $[NEt_4](ClO_4)$–CH_3CN. Possible origins for the nonexponential decay behavior have been discussed previously.[1] By combining the concentrating effect in the films and the spread in τ values, $k_q = 3.3 \times 10^8$–2.0×10^9 M^{-1} s^{-1}. This range is within a factor of ~10 of the diffusion-controlled limit in many polar organic solvents. Diffusion of PQ^{2+} to the chromophoric sites that produce

---

(10) Dressick, W. J.; Meyer, T. J.; Durham, B. *Isr. J. Chem.* **1982**, *22*, 153.

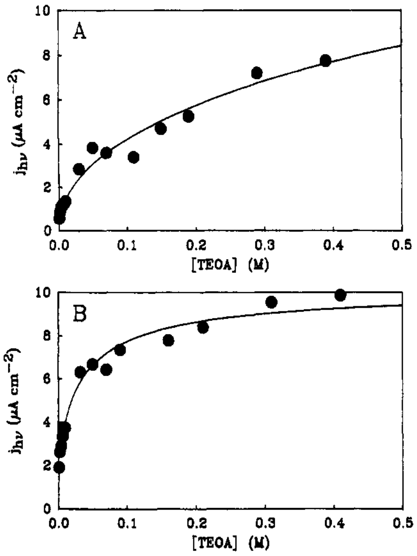

Figure 5. Plot of $j_{h\nu}$ vs [TEOA]. As in Figure 2 with $[PQ^{2+}] = 0.25$ mM (A) with 0.1 M TEAP-CH_3CN as the external medium. The line through the data points is the function $B_1/[1 + (1 + B_2/[TEOA])^{1/2}]$ with $B_1 = 51 \pm 33$ and $B_2 = 12 \pm 18$ (note eq 19). (B) With 0.1 M isopropyl alcohol also present; $B_1 = 20 \pm 1$ and $B_2 = 0.16 \pm 0.04$.

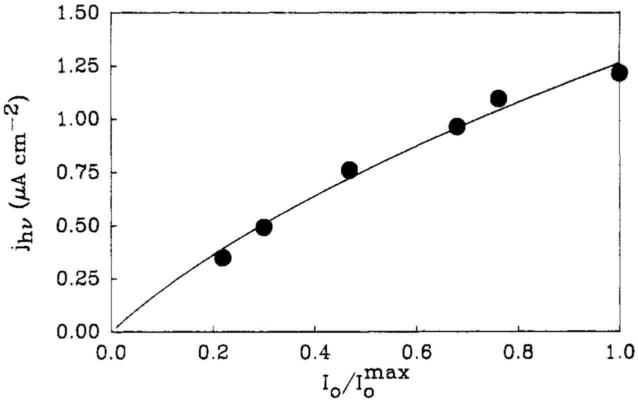

Figure 6. Plot of $j_{h\nu}$ vs I_0/I_0^{max}, $I_0^{max} \sim 10^{-9}$ einstein cm^{-2} s^{-1}. In 0.1 M TEAP-CH_3CN with [TEOA] = 100 mM and $[PQ^{2+}] = 0.25$ mM. The line is the function $X_1(-1 + [1 + X_2(I_0/I_0^{max})]^{1/2})$ with $X_1 = 0.86 \pm 0.39$ and $X_2 = 5.1 \pm 3.1$ (note eq 19).

the photocurrent is clearly a rapid process.

Variations with Light Intensity and [TEOA]. Once formed by oxidative quenching, Ru(III) is reduced to Ru(II) either by TEOA or by PQ^+. Capture by PQ^+ is a deleterious "recombination" step since it depletes the reductive carrier. Kinetically, the competition between PQ^+ and TEOA for Ru(III) links the photoproduction of PQ^+ with its transport to the electrode. It is this linkage that causes the complex relationship among $j_{h\nu}$, I_0, and [TEOA] in eq 15.

The variations of $j_{h\nu}$ with [TEOA] and I_0 in Figures 5 and 6 demonstrate that eq 15 is correct, at least in form. In Figure 5 are shown plots of $j_{h\nu}$ in μA cm^{-2} vs [TEOA]. The line in Figure 5 is a plot of $j_{h\nu}$ against the function $B_1/[1 + (1 + B_2/[TEOA])^{1/2}]$. From eq 15 the constants B_1 and B_2 are defined as

$$B_1 = \frac{nFD_{PQ^+}}{x}C_1I_0 \tag{19a}$$

$$B_2 = C_2I_0 \tag{19b}$$

The results of two experiments are shown in Figure 5, one in the presence of 0.1 M isopropyl alcohol. In both cases, $j_{h\nu}$ shows the expected bendover at high [TEOA]. The bend-over occurs more sharply and at lower [TEOA] in the presence of isopropyl alcohol. The ratios B_1/B_2 for the fits shown in Figure 5 are 4.2 and 130 in the absence and presence of 0.1 M isopropyl alcohol, respectively. The effect of added isopropyl alcohol is obviously important.

The variations of $j_{h\nu}$ with the ratio I_0/I_0^{max} is shown in Figure 6. I_0^{max} is the maximum light intensity used in a series of experiments. The line in Figure 6 is a plot of $j_{h\nu}$ against the function $X_1(-1 + [1 + X_2(I_0/I_0^{max})]^{1/2})$ at constant [TEOA]. From eq 15, X_1 and X_2 are defined as

$$X_1 = \frac{nFD_{PQ^+}k_s[TEOA]}{2k_bx} \tag{19c}$$

$$X_2 = C_2/[TEOA] \tag{19d}$$

The plot in Figure 6 shows the expected bend-over in photocurrent density as the light intensity is increased from $\sim 2 \times 10^{-10}$ to 10^{-9} einstein cm^{-2} s^{-1}.

Separation Efficiency. Per Photon Absorbed Efficiency of the Photoelectrode. The per photon absorbed quantum yield of the photoelectrode, $\phi_{h\nu}$, can be defined by eq 20 as the fraction of current equivalents produced per photon absorbed:

$$\phi_{h\nu} = j_{h\nu}/nFI_0(1 - 10^{-A_T})(A_{Ru}/A_T) \tag{20}$$

At high concentrations of [TEOA] and low light intensities almost all of the PQ^+ produced photochemically is captured at the inner electrode. Under these conditions the term containing C_2 in eq 15 is negligible. $\phi_{h\nu}$ is related to the quantum yield for the photoproduction of oxidative and reductive equivalents, ϕ_p, by

$$\phi_p = \phi_q\phi_{sep} = \phi_{h\nu}/F \tag{21}$$

In eq 21 F is the fraction of absorbing chromophores that lead to photocurrent, i.e., those sites that are rapidly quenched. ϕ_q was defined in eq 16.

Quenching occurs by diffusion of PQ^{2+} to the excited state followed by electron transfer:[4e,11]

$$\xrightarrow{h\nu} (bpy)_2Ru^{III}(5\text{-}NH(SO_2\text{–}PS)phen^{\bullet-})^{2+*} + PQ^{2+} \underset{k_{-D}}{\overset{k_D}{\rightleftharpoons}} [(bpy_2)Ru^{III}(5\text{-}NH(SO_2\text{–}PS)phen^{\bullet-})^{2+*},PQ^{2+}] \tag{22}$$

$$[(bpy)_2Ru^{III}(5\text{-}NH(SO_2\text{–}PS)phen^{\bullet-})^{2+*},PQ^{2+}] \xrightarrow{k_{ox}} [(bpy_2)Ru^{III}(5\text{-}NH(SO_2\text{–}PS)phen)^{3+},PQ^{\bullet+}] \tag{23}$$

Following the electron-transfer quenching step, there is a competition between separation of the redox products and back electron transfer before separation can occur:

$$\begin{tikzcd}
(bpy)_2Ru^{III}(5\text{-}NH(SO_2\text{-}PS)phen)^{3+} + PQ^{\bullet+} \\
{[(bpy)_2Ru^{III}(5\text{-}NH(SO_2\text{-}PS)phen)^{2+},PQ^{\bullet+}]} \arrow[u, "k_1"] \arrow[d, "k_2"'] \\
{[(bpy)_2Ru^{II}(5\text{-}NH(SO_2\text{-}PS)phen)^{2+},PQ^{2+}]}
\end{tikzcd} \tag{24}$$

If the reverse of reaction 23, back electron transfer to give the excited state, is unimportant, the constants k_q and ϕ_{sep} of reaction 4 in Scheme I are defined by

$$k_q = \frac{k_{ox}k_D}{k_{-D} + k_{ox}} \tag{25}$$

$$\phi_{sep} = \frac{k_1}{k_1 + k_2} \tag{26}$$

The separation efficiency, ϕ_{sep}, is the fraction of quenching events that produce separated, uncorrelated redox equivalents. *The product $F\phi_{sep}$ represents the maximum efficiency with which the photoelectrode can operate under these conditions.*

In the utilization of photocurrent measurements and eq 19 to estimate $\phi_{h\nu}$, a potential complication arises from the fact that $PQ^{\bullet+}$ is a significant visible light absorber ($\epsilon_{605nm} = 10060$ M^{-1} cm^{-1}).[12] If it reaches a high concentration at the photoelectro-

---

(11) (a) Rehm, D.; Weller, A. *Ber. Bunsen-Ges. Phys. Chem.* **1969**, *73*, 834. *Isr. J. Chem.* **1970**, *8*, 259. (b) Kosower, E. M.; Cotter, J. L. *J. Am. Chem. Soc.* **1964**, *86*, 5524.

chemical steady state, the fraction A_{Ru}/A_T could become significantly less than 1. The photolysis wavelength (436 nm) is a region of minimum light absorptivity for $PQ^{\bullet +}$. In addition, the magnitudes of the photocurrents suggest that the steady-state concentration of PQ^+ is relatively low. For a photocurrent density of 10 μA cm^{-2}, a film thickness of 1000 Å, and $D = 10^{-5}$ cm^2 s^{-1}, it can be estimated that $[PQ^+]_{PSS} \leq 10^{-6}$ M by using eq 12. This calculation assumes a limiting case where the diffusion layer extends across the entire film.

Actinometry measurements were carried out by using a 200-W Hg lamp. On the basis of a series of separate experiments using ferrioxalate actinometry, the value of I_0 was found to be $(6.6 \pm 0.8) \times 10^{-9}$ einstein cm^{-2} s^{-1} during the course of the quantum yield measurements. Actinometry and photocurrent measurements were carried out sequentially to minimize the effects of lamp variations. The relatively large error in I_0 is due largely to the difficulties that arise in placing the cell in the same part of the photolysis beam between sequential photocurrent and actinometry experiments (Figure 1A). An estimate of $A_{Ru} = 0.067$ was made for films prepared by soaking in the $[(bpy)_2Ru(5\text{-}NH_2phen)]^{2+}$-containing solution for 2 h. As noted below, films soaked for this period give a maximal photocurrent response. The estimate was based on optical density measurements on films that had been cast on semitransparent platinized glass substrates.

A series of quantum yield measurements was made on films that had been soaked for 2 h in the $[(bpy)_2Ru(5\text{-}NH_2phen)]^{2+}$-containing solution and with 60 mM TEOA and 0.25 mM PQ^{2+} in the external solution during the photolysis period. From the measured value of I_0, the results of steady-state photocurrent measurements, and the assumption that absorbance by PQ^+ is negligible ($A_T \sim A_{Ru}$), $\phi_{h\nu} \geq 0.06 \pm 0.04$ was calculated by using eq 19.

$\phi_{h\nu}$ was calculated by assuming that light reaching the electrode surface was 100% reflected and is reabsorbed as it passes back through the film. To include the effect, at our low light-absorbance levels the value of A_{Ru} used in eq 19 was twice the experimental value. If there are reflection losses, $\phi_{h\nu}$ is a lower limit. $\phi_{h\nu}$ may be artifically high by a factor as large as 2 if, rather than undergoing disproportionation (reaction 10), the oxidized TEOA radical is further oxidized by PQ^{2+} to give PQ^+. In that case there would be a "boost" in the observed photocurrent arising from the production of a second PQ^+ per photon absorbed.

In an initial communication a value of $\phi_{h\nu} = 0.03$ was reported under similar conditions.[2a] The earlier value was obtained at lower concentrations of TEOA and before a full appreciation of the role of the distribution of the chromophore within the films was available, see below.

From the data in Figure 5, relative to the point at [TEOA] = 60 mM where $\phi_{h\nu} = 0.06 \pm 0.04$, $\phi_{h\nu}$ is 0.14 at [TEOA] = 0.4 M and is 0.18 with 0.1 M isopropyl alcohol added as well. These are the highest per photon absorbed quantum yields that were reached in our experiments.

Experimentally, we were unable to reach conditions where the term containing C_2 in eq 15 is negligible, $\phi_{h\nu}$ is, therefore, a complex function of I_0, [TEOA], and ϕ_p. From our data it is possible to estimate a lower limit for ϕ_p and, under conditions where ϕ_q is known, a lower limit for ϕ_{sep} as well. The appropriate relation is

$$\phi_{sep} > \phi_{h\nu}/F\phi_q \tag{27}$$

The lower limit is a consequence of the fact that even at our highest concentrations of added TEOA the condition $C_2I_0/[TEOA] \rightarrow 0$ has not yet been reached. Recombination by back electron transfer still plays a role in determining the magnitude of $\phi_{h\nu}$.

The fraction of absorbing sites that contribute to the photocurrent, F, is unknown. Lifetime quenching experiments in the presence of added PQ^{2+} and TEOA (50 mM) show that ~74% of the light emitted from the films comes from photocurrent-producing sites.[1] However, because of differences in radiative and nonradiative decay rate constants among the three different sites, the fraction of light emitted is *not* a direct measure of their fractional content within the films.

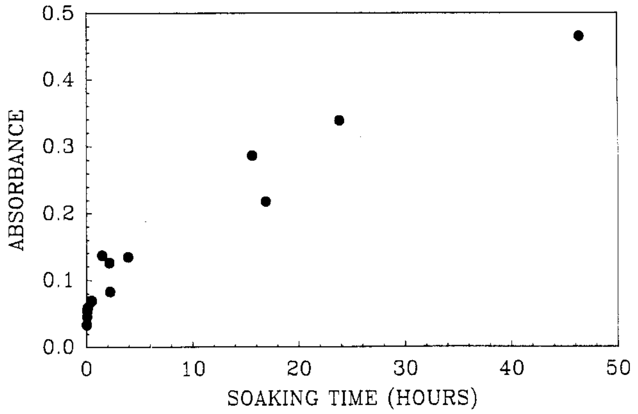

Figure 7. Absorbance of $PS\text{-}SO_2Cl$ films at 455 nm as a function of soaking time in an acetonitrile solution 5 mM in $[(bpy)_2Ru(5\text{-}NH_2phen)](PF_6)_2$. The absorbance measurements were made after the films were dissolved in 1 mL of dimethyl sulfoxide. Films were cast onto 4.5-cm^{-2} glass slides by using 360 μL of an acetone solution containing 0.4 mg/mL of the $PS\text{-}SO_2Cl$ polymer.

In any case, with $\phi_q = 0.87$ at $[PQ^{2+}] = 0.25$ mM (Figure 4), $\phi_{h\nu} = 0.14$ at [TEOA] = 0.4 M, and $F = 1$, $\phi_{sep} > 0.16$. This value is comparable to values obtained for the quenching of $[Ru(bpy)_3]^{2+*}$ and related excited states by PQ^{2+} in water or in polar organic solvents.[12-14]

Structural Effects. Variations in Photocurrent with the Concentration Gradient of the Chromophore. The total concentration of metal complex chemically bound within the films can be varied by increasing the exposure time of the precast films to an acetonitrile solution containing $[(bpy)_2Ru(5\text{-}NH_2phen)]^{2+}$. The point is demonstrated in Figure 7 where the absorbance at 455 nm as a function of soaking time is plotted. So that the quantity of material used in the measurements could be increased, relatively large area films were used, and so that potential complications arising from film inhomogeneities could be avoided, the absorbance measurements were made by dissolving the films in dimethyl sulfoxide (DMSO) solution.

From the data in Figure 7 the chromophore uptake is initially rapid but becomes progressively slower as more complex is bound. A similar absorbance–time curve was also obtained for spun-cast films on semitransparent glass/platinum substrates where the absorbance values were measured by direct transmission measurements on the intact films. Curves similar to the one shown in Figure 7 have been observed in related heterogeneous systems where the rate of a reaction is limited by mass transfer of a reactant into or through a polymeric substrate.[15]

In certain cases the time dependence has been successfully modeled, giving information concerning the rate-determining step of the overall process and the spatial distribution of the reactant in the resulting chemically modified structure. If diffusion of the reactant through a region where it is already chemically bound is rate determining, a concentration gradient is expected to form. In the concentration gradient the chromophore level is high on the outside at the film–solution interface and decreases toward the inside of the film. We have been unable to obtain satisfactory fits of the data in Figure 7 to available models. The scatter in the data is too great, and there is a large uncertainty in absorbance at $t = \infty$, which is a necessary quantity for the analyses. However, the qualitative appearance of the absorbance vs soaking time curve in Figure 7 is consistent with formation of a concentration gradient

---

(12) (a) Hoffman, M. Z.; Prasad, D. R. *NATO ASI Ser. C* **1987**, *214*, 153. (b) Prasad, D. R.; Mandal, K.; Hoffman, M. Z. *Coord. Chem. Rev.* **1985**, *64*, 175.

(13) (a) Olmsted, J., III; Meyer, T. J. *J. Phys. Chem.* **1987**, *109*, 3287. (b) Maestri, M.; Sandrini, D. *Nouv. J. Chim.* **1981**, *5*, 637.

(14) Chou, S. F.; Chou, M.; Creutz, C.; Matsubara, T.; Sutin, N. *J. Am. Chem. Soc.* **1981**, *103*, 369.

(15) (a) Schmuckler, G. *React. Polym.* **1984**, *2*, 103. (b) Streat, M. *React. Polym.* **1984**, *2*, 79. (c) *Ion Exchange and Solvent Extraction*; Marinsky, J. A., Marcus, Y., Eds.; Marcel Dekker: New York, 1977; Vol. 7, Chapter 1. (d) Carter, R. E. *J. Chem. Phys.* **1961**, *34*, 2010.

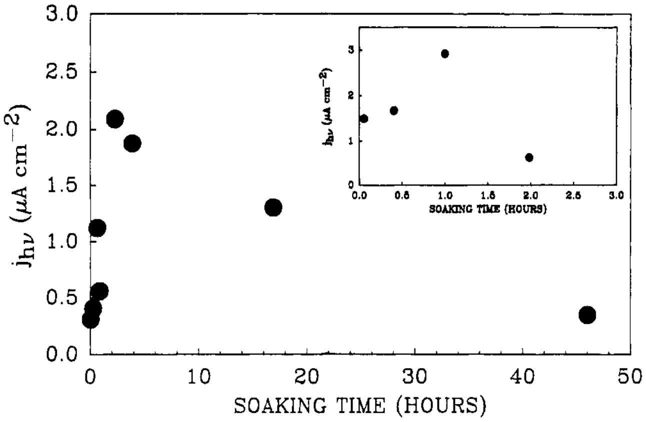

Figure 8. Variation in $j_{h\nu}$ in μA/cm^2 with soaking time. Evaporatively cast PS–SO_2Cl films on 0.125-cm^2 electrodes were exposed to an external solution containing 5 mM [$(bpy)_2Ru(5\text{-}NH_2phen)$][$PF_6$]$_2$ in acetonitrile. λ_{exc} = 455 nm; the external solution was 60 mM in TEOA and 0.25 mM in PQ^{2+}. In the inset are shown photocurrents generated from spun-cast films treated in the same manner.

of chromophore within the films, with the concentration of chromophore being highest at the film–solution interface.

The spatial distribution of the chromophore within the films has been investigated by using the SIMS/ion microprobe technique. The complete details of the experiment have been published elsewhere.[7] In brief, it involves sputtering through the polymer with an O_2^+ ion beam 1 μm in diameter rastered over a 250-μm^2 area while monitoring the mass spectrum of secondarily emitted ions in the Ru^+ region. The technique was used to obtain depth-resolved concentration profiles of the Ru content in PS–SO_2Cl films that had been soaked in chromophore-containing solutions for various times.

The resulting mass spectra verify that Ru is present in films soaked for periods as short as 1–2 min. Two-dimensional mapping of the film surfaces showed that within the 1-μm resolution of the ion microprobe the distribution of Ru is homogeneous laterally. Unfortunately, vertical depth profiles toward the electrode lack sufficient resolution to define the concentration gradient of the chromophore within the films in any detail. However, they do show that the majority of the chromophore is concentrated toward the outside of the films, away from the electrode–film interface after short soaking times.

Photoelectrochemical measurements (455 nm) were carried out on films on Pt electrodes prepared in exactly the same way as those used in the absorbance measurements. The concentration of PQ^{2+} (0.25 mM) in the external 0.1 M TEAP–CH_3CN solution was sufficiently high that $\phi_q \sim 0.87$ and the concentration of TEOA was held at 60 mM. As shown in Figure 8, maximum photocurrents were obtained for evaporatively cast films that had been soaked in the chromophore-containing solution for 1–2 h and for the spun-cast films at a soaking time of ~1 h as shown in the inset. The results show that $j_{h\nu}$ depends upon the soaking time and, by inference, upon the distribution of the chromophore within the films.

To obtain photocurrents and photocurrent densities on a per photon absorbed basis, we divided the experimental current densities by a measure of the light absorbed $(1 - 10^{-A_{Ru}})$ by using the absorbance data in Figure 7. The absorbance values were obtained in a separate series of experiments as described above. The resulting normalized current densities were used to calculate $\phi_{h\nu}$ relative to $\phi_{h\nu} = 0.06 \pm 0.04$, which was measured at a soaking time of 2 h as described above. The variations in both quantities as a function of soaking time are shown plotted in Figure 9.

The dramatic increase and decrease in $\phi_{h\nu}$ between 1 and 2 h under conditions where ϕ_q is close to 1 is a notable feature of the data. The same result was obtained in qualitative detail when the experiment was repeated by using the morphologically more homogeneous spun-cast films.

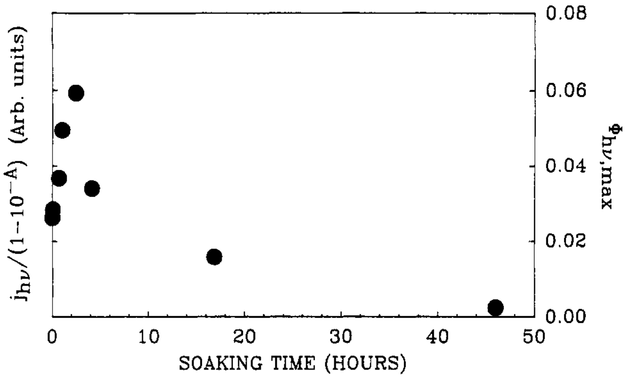

Figure 9. As in Figure 8 but a plot of $j_{h\nu}/(1 - 10^{-A_{Ru}})$ vs soaking time. The points were calculated by using the data in Figure 8 and absorbance values taken from the curve shown in Figure 7. Per photon absorbed quantum yields for photocurrent production are shown on the right-hand abscissa. They are not maximum quantum yields because of the relatively low concentration of TEOA in the external solution.

In Figure 10 are shown a series of cyclic voltammograms obtained on films to which the chromophore had been attached by varying the soaking times from 1 min to 3.5 h. In scans from 0 to +1.50 V, the expected Ru(III/II) couple appears at $E_{1/2}$ = 1.42 V but only after soaking periods of ~2 h or longer. A soaking time of 2 h coincides with the photocurrent maximum in Figure 9. This 2-h soaking period is required even though the data in Figure 7 show that the complex is present in the film in significant amounts after soaking periods as short as 1–2 min. The appearance of the Ru(III/II) couple in cyclic voltammograms of the smooth, spun-cast polymeric films also coincides with the point of maximum photocurrent efficiency.

Discussion

The combination of results presented by the earlier lifetime and emission measurements[1] and the photoelectrochemical experiments described here allows relatively clear physical models to be constructed of the interior structure of the films and of the mechanisms by which photocurrents arise. The lifetime and emission measurements probe the dynamics of the quenching event at their source, the chromophore. The photocurrent measurements rely on diffusional capture of the photoproduct, PQ^+, at the spatially remote inner electrode. The magnitude of $j_{h\nu}$ depends upon the quenching, separation, and scavenging events collected in Scheme I.

The laser flash photolysis experiments in the presence of added quencher establish that the chromophore occupies three chemically different sites after the hydrolysis step. The coincidence of K_{SV} values between the quenching and photocurrent measurements and the independence of both on added [NEt_4](ClO_4) show that *only the "rapidly" quenched component contributes to the photocurrent.* That only a fraction of the available chromophores lead to photocurrent makes the maximum per photon absorbed quantum yields for photocurrent production of ~0.14 at [TEOA] = 0.4 M even more impressive.

It was suggested earlier that the sites that are rapidly quenched reside near $-SO_3^-$-based ion-exchange incursion channels created in the hydrolysis step.[1] The ion channels serve two roles. They provide a basis for rapid diffusion of PQ^{2+} to the excited states and a facile conduit for PQ^+ to return to the normal translation channels by which the $PQ^{2+/+}$ couple diffuses to the electrode. The extent of hydrolysis may be small, as shown by IR, but the ion channels are required for significant photocurrents to appear.

The observation of Stern–Volmer kinetics for quenching by PQ^{2+} in both the emission and photocurrent measurements shows that the quenching process is diffusional and not static in nature. By the same token, variations in photocurrent with both [TEOA] and light intensity are in accord with the kinetic model derived from Scheme I. The agreement substantiates the diffusional capture of Ru(III) by competitive electron transfer from TEOA or PQ^+. We have no quantitative information concerning the partitioning of TEOA between the film and the external solution, but as shown by the data in Figure 5, relatively high concentrations of TEOA must be reached before reduction by PQ^+ is negligible.

The amount of TEOA required to approach the region of complete capture by TEOA is reduced considerably in the presence of added isopropyl alcohol (Figure 5B). The effect of the added alcohol as a plasticizer may be dynamic in increasing k_s at the expense of k_b. The alcohol may also increase the partition coefficient for TEOA within the film by swelling the membrane.

For the quenching step the magnitude of the Stern–Volmer quenching constant ($K_{SV} \sim 2.3 \times 10^4$ M^{-1}) is remarkably high. Even when the concentrating effect within the hydrolyzed films is included ($K_p \sim 10^2$), the quenching rate constant ($k_q \sim (0.3–2) \times 10^9$ M^{-1} s^{-1}) is comparable in magnitude to that found for the quenching of $Ru(bpy)_2(5\text{-}NH_2phen)^{2+*}$ by PQ^{2+} in 0.1 M TEAP–CH_3CN ($k_q = 2.8 \times 10^9$ M^{-1} s^{-1}).[16] The latter value is within a factor of 10 of the diffusion-controlled limit in CH_3CN. The magnitude of k_q is impressive when note is taken of the fact that inhibition to diffusion by factors of 10^4–10^7 have been observed for redox couples in ion-exchange membranes like Nafion.[17]

The environments around the chromophoric sites dictate their abilities to contribute to the photocurrent in other ways as well. As noted above, at the rapidly quenched sites the separation efficiency, $\phi_{sep} > 0.16$, is comparable to values obtained in solution. ϕ_{sep} is the maximum photocurrent efficiency that can be obtained at the photoelectrode. The magnitude of ϕ_{sep} is determined by the rate constants for separation and back electron transfer as shown in reaction 24. They respond differently to different factors.[12-14] Separation is promoted by electrostatic repulsion between the initially formed Ru^{3+},PQ^+ photoproducts and by medium effects in general. Spin effects and the amount of energy released help to dictate the rate of back electron transfer. Although there are too many factors to make a quantitative accounting, the local film environment near the excited states is at least comparable to a polar solvent in promoting separation.

There are two additional sites occupied by the chromophores, neither of which contributes to the photocurrent. One site apparently lies deeply buried within a hydrophobic, relatively crystalline region of the film and is not quenched. A second site is quenched, but slowly, and even then only in the presence of added $[NEt_4](ClO_4)$. These sites may lie in a hydrophobic region away from the ion channels where diffusion of the $PQ^{2+/+}$ couple is slow. Their inability to contribute to the photocurrent may be a consequence of slow diffusion of the $PQ^{2+/+}$ couple near these sites, thus enhancing back electron transfer over separation following the quenching step.

Dependence of $i_{h\nu}$ on the Concentration Gradient. From the data in Figures 8 and 9, the photocurrent and $\phi_{h\nu}$ are strongly dependent upon the soaking time and, by inference, on the structural details of how the chromophoric sites are arrayed within the films. The absorbance–soaking time curve in Figure 7 and the ion microprobe/SIMS experiments[7] show that the chromophore is spatially isolated in the outside of the films at short soaking times. The chromophore enters the films with the formation of a concentration gradient with the gradient decreasing from the film–solution interface into the interior of the film. At longer soaking times as the chromophore penetrates further into the films, $j_{h\nu}$ rises dramatically (×7) and $\phi_{h\nu}$ less so (×2). Maximum values for both are reached at ~2 h. Past 2 h both $j_{h\nu}$ and $\phi_{h\nu}$ fall dramatically even though the amount of light absorbed by the films increases steadily.

The origin of the decrease in $\phi_{h\nu}$ past a soaking time of 2 h is to be found in the cyclic voltammograms in Figure 10. Significant amounts of chromophore are incorporated into the film even at the earliest soaking times. However, the Ru(III)/(II) couple appears at the electrode only after ~2 h, which coincides with the maximum value that $\phi_{h\nu}$ reaches as a function of soaking time.

The electrochemical response of the Ru couple arises by oxidation of Ru(II) to Ru(III) near the film–electrode interface. Oxidation at the electrode followed by site-to-site electron-transfer hopping eventually leads to complete oxidation of Ru(II) to Ru(III) throughout the film:[18]

$$Pt|{\sim}Ru^{II}_{inner}{\sim}\,{\sim}Ru^{II}_{outer} \xrightarrow{-e^-} Pt|{\sim}Ru^{III}_{inner}{\sim}\,{\sim}Ru^{II}_{outer} \rightarrow Pt|{\sim}Ru^{II}_{inner}{\sim}\,{\sim}Ru^{III}_{outer}$$

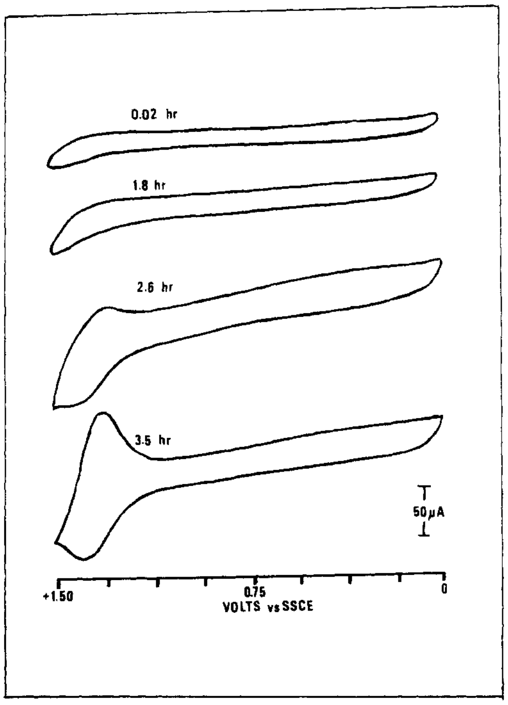

Figure 10. Cyclic voltammograms of $PS–SO_2Cl$ films at various soaking times as in Figure 8. Films were cast by using the same conditions as in Figure 4, rinsed in clean MeCN and soaked in 0.1 M TEAP/acetonitrile prior to the electrochemical measurements. The external solution contained 0.1 M TEAP –CH_3CN.

For the electron-transfer channel to open, there is a requirement that the couple reach the electrode–film interface. After a 2-h soaking period, there is a sufficiently high concentration of Ru(II) sites near the electrode surface to lead to a measurable voltammetric response. At soaking times past 2 h the voltammetric wave shape becomes more nearly reversible and the peak current increases. The peak current is enhanced because the number of Ru(II) sites is increasing. The enhanced reversibility results from a buildup in Ru(II) sites near the electrode–film interface. The buildup further develops the electron-transfer channel and increases the electron-hopping rate.

The appearance of the Ru(III/II) electron-transfer channel has a deleterious effect on $j_{h\nu}$. In the photocurrent experiment the potential of the electrode is held between the potentials of the $PQ^{2+/+}$ and Ru(III)/(II) couples. At these potentials, oxidation of PQ^+ occurs and is the basis for the photocurrent:

$$PQ^+ \xrightarrow[k_\alpha]{-e^-} PQ^{2+}$$

However, both PQ^+ and Ru(III) are produced following the quenching–separation steps. The actual photocurrent obtained will be diminished to the extent that reduction of Ru(III) also occurs at the electrode (Scheme I):

$$\text{Ru(III)} \xrightarrow[k'_\alpha]{+e^-} \text{Ru(II)}$$

In a kinetic sense, the appearance of the Ru(III/II) channel presents an additional competition for Ru(III), now between TEOA, PQ^+, and the electrode (k'_{ct} in Scheme I). The channel can be included in a straightforward manner in a more general

---

(16) (a) Margerum, L. D. Ph.D Thesis, University of North Carolina at Chapel Hill, NC 27514. (b) McClanahan, S. F., unpublished results.

(17) (a) Buttry, D. A.; Anson, F. C. *J. Am. Chem. Soc.* **1983**, *105*, 1505. (b) Montgomery, D. D.; Anson, F. C. *J. Am. Chem. Soc.* **1985**, *107*, 3431.

(18) (a) Kaufman, F. B.; Engler, E. M. *J. Am. Chem. Soc.* **1979**, *101*, 547. (b) Kaufman, F. B.; Schroeder, A. H.; Engler, E. M.; Kramer, S. R.; Chambers, J. Q. *Ibid.* **1980**, *102*, 483.

kinetic analysis based on Scheme I. Qualitatively, a comparison of the data in Figures 9 and 10 shows that the fall in $\phi_{h\nu}$ from ~2- to ~4-h soaking times is paralleled by an increase in the integrated current for the Ru(III)/(II) couple. As the electron-transfer channel becomes more fully developed, reduction of Ru(III) at the electrode becomes competitive with reduction by TEOA and both $j_{h\nu}$ and $\phi_{h\nu}$ fall.

An additional factor that may contribute to the decrease in $\phi_{h\nu}$ with soaking times is energy-transfer quenching by the electrode. Energy-transfer quenching would occur by excitation and energy migration to the electrode–film interface:

$$\mathrm{Pt}|{\sim}\mathrm{Ru^{II}}_{\mathrm{inner}}{\sim}{\sim}\mathrm{Ru^{II}}_{\mathrm{outer}} \xrightarrow{h\nu} \mathrm{Pt}|{\sim}\mathrm{Ru^{II}}_{\mathrm{inner}}{\sim}{\sim}\mathrm{Ru^{II*}}_{\mathrm{outer}} \rightarrow \mathrm{Pt}|{\sim}\mathrm{Ru^{II*}}_{\mathrm{inner}}{\sim}{\sim}\mathrm{Ru^{II}}_{\mathrm{outer}}$$

If it is important, such an energy-transfer channel would also be triggered when the $\mathrm{Ru^{II}}$ sites reach the electrode surface.

The photocurrent and to a lesser extent $\phi_{h\nu}$ initially rise with soaking time. Similar effects have been noted by Morishima et al., where variations in photocurrents were observed to occur as the thickness of an underlying quencher film was varied,[19] and by Deronizer et al., who observed a photocurrent maximum in a related experiment.[20] The effect is far more dramatic in the evaporatively cast films than it is in the smoother, spun cast films (Figure 8).

The initial rise in photocurrent is also a structural consequence of the changes that occur in the concentration gradient as the soaking time is increased. By the nature of the molecular photochemical apparatus, the photocurrent carrier, $\mathrm{PQ^+}$, is produced at the Ru(II) sites within the bulk of the films. Ru(II) penetrates further into the films at longer soaking times, and the average distance traversed by the photocurrent carrier is decreased. At early soaking times, the diffusion distance for $\mathrm{PQ^+}$ is large. The majority of chromophores and quenching events occur well away from the electrode–film interface. As the electrode is approached, the average distance traversed decreases, thus increasing $j_{h\nu}$. In terms of the simple linear diffusion model upon which eq 12 is based, the effective thickness of the diffusion layer, x, is decreased as Ru(II) penetrates into the films.

At least qualitatively, the increase in $[\mathrm{PQ^+}]/x$ with soaking time helps to explain the approximately 7-fold increase in $j_{h\nu}$ as the soaking time is increased to 2 h. It does not explain the approximately 2-fold increase in $\phi_{h\nu}$. $\phi_{h\nu}$ is determined by the molecular photochemical apparatus. It depends upon the competition between TEOA and $\mathrm{PQ^+}$ for Ru(III) and the partitioning and diffusional characteristics of TEOA and of the $\mathrm{PQ^{2+/+}}$ couple.

The initial increase in $\phi_{h\nu}$ with soaking time is probably a medium effect. It could arise from changes induced in the microenvironment of the film by the chemical binding of the large ($r \sim 7$ Å) cationic Ru(II) complex. As the local concentration of cationic complexes rises, the change in local environment may affect $\phi_{h\nu}$ by (1) increasing the number of sites that are rapidly quenched, (2) increasing the local quenching rate constant, (3) increasing k_1 at the expense of k_2, thus enhancing ϕ_{sep}, (4) enhancing the partitioning or diffusional characteristics of TEOA within the film, or (5) some combination of 1–4.

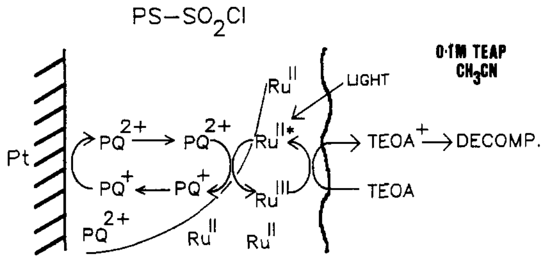

Figure 11. Schematic representation of the events occurring within the polymeric films following excitation. No attempt is made in the illustration to represent the translational or ion incursion channels for the $\mathrm{PQ^{2+/+}}$ couple; however, note Figure 11 in ref 1. The concentration gradient of $[(\mathrm{bpy})_2\mathrm{Ru}(5\text{-}\mathrm{NH}(\mathrm{SO_2}\text{–}\mathrm{PS})\mathrm{phen})]^{2+}$ is shown.

Presumably, the origin of the increase in $\phi_{h\nu}$ would become more obvious by carrying out photocurrent measurements as a function of $[\mathrm{PQ^{2+}}]$, [TEOA], and I_0 at the shorter soaking times. At the present time, however, the reduced photocurrent magnitude at the shorter soaking times makes such a study impractical.

Role of the Concentration Gradient. An illustration of the microstructural array of the components of the molecular photochemical apparatus within the films is shown in the cartoon in Figure 11. The concentration gradient of chromophores within the films imparts an interior structure and, because of it, an inherent rectification or directed charge-transfer character. Reductive equivalents are delivered to the interior of the films via the $\mathrm{PQ^{2+/+}}$ couple and oxidative equivalents to the immobile, Ru(III) sites which are held in fixed positions in the exterior of the films.

The concentration gradient–photochemical apparatus is not a true photodiode. Reductive equivalents are collected at the inner electrode as $\mathrm{PQ^+}$, but the oxidizing equivalents (as Ru(III)) are accessible only by the diffusion of a chemical reductant into the films. The success of TEOA as a reductive scavenger lies in its ability to penetrate into and diffuse through the film to the Ru(III) sites.

The possibility exists that the PS–SO$_2$Cl films can be redesigned both to achieve higher quantum efficiencies and, more importantly, to achieve true separation of the photochemically produced reductive and oxidative equivalents, one to the interior and one to the exterior of the films. The key is in the design of even more complex molecular arrays within the film structure, a theme that is currently under investigation.

Acknowledgments are made to the Department of Energy under Grant No. DE-FG05-86ER13633 for support of this research.

Registry No. $\mathrm{PQ^{2+}}$, 4685-14-7; TEOA, 102-71-6; Pt, 7440-06-4; isopropanol, 67-63-0.

---

[19] Morishima, Y.; Fukushima, Y.; Nozakura, S. *J. Chem. Soc., Chem. Commun.* **1985**, 912.

[20] Cosnier, S.; Deronzier, A.; Moutet, J.-C. *J. Phys. Chem.* **1985**, *89*, 4895.